

Photodissociation spectroscopy of phenol dimer ion. Lack of resonance interaction between the aromatic rings

Kazuhiko Ohashi[#], Yoshiya Inokuchi[#], Nobuyuki Nishi[#]

*Department of Chemistry, Faculty of Science, Kyushu University,
Hakozaki, Fukuoka 812-81, Japan*

Abstract

Electronic spectra of a homo-molecular but inequivalent dimer ion, $(\text{C}_6\text{H}_5\text{OH})_2^+$, are measured by photodissociation spectroscopy. A broad band appeared in the 340–440 nm region is characteristic of the $\text{C} \leftarrow \text{X}$ transition of a phenol ion chromophore, suggesting that the dimer ion consists of a phenol ion and a neutral phenol. No strong band is observed in the 450–1400 nm region, whereas other aromatic dimer ions usually show charge resonance bands in near-infrared region. Owing to the geometrical constraint of an $\text{O}-\text{H}\cdots\text{O}$ hydrogen bond in $(\text{C}_6\text{H}_5\text{OH})_2^+$, the two aromatic rings cannot be in a parallel configuration suitable for the resonance interaction.

[#] Present address: Institute for Molecular Science, Myodaiji, Okazaki 444, Japan.

1. Introduction

Studies of molecular van der Waals clusters and cluster ions have provided insight into the nature of intermolecular interactions. Photodissociation of mass-selected cluster ions has been a useful technique in cluster ion spectroscopy [1]. The method employs tandem mass filter arrangements which isolate specific cluster ions for photodissociation and analyze the mass number of the resultant fragments [2]. In a series of previous studies with this technique, we measured electronic spectra of homo-dimer ions of several aromatic molecules, including benzene [3,4], toluene [5] and naphthalene [6]. For each homo-dimer ion, a charge resonance (CR) band is much stronger than a local excitation (LE) band, indicating that the two component molecules are equivalent to each other and that the positive charge is equally shared with the two molecules (charge delocalization). Since the CR band is due to the resonance interaction between the π electron systems belonging to the two aromatic rings, a parallel configuration is expected for the dimer ions rather than a T-shape configuration.

Here a question arises whether the resonance interaction found in the homo-dimer ions can be also seen in dimer ions in which the two component molecules are inequivalent to each other. One class of such species is hetero-dimer ions composed of a benzene and a substituted benzene. These hetero-dimer ions are likely less stable than the homo-dimer ions because stabilization energy due to the charge delocalization is expected to decrease with increasing difference in the ionization energies (IEs) between the two molecules [7]. However, we have found that the spectrum of (benzene \cdots toluene)⁺ shows absorption bands which are best ascribed to the resonance-type interaction between the two aromatic rings [8].

Phenol dimer ion, as well as neutral phenol dimer, is a different example of inequivalent dimers. Multiphoton ionization (MPI) spectroscopy of the neutral dimer suggested that the species has an O–H \cdots O hydrogen bond [9,10]. Two origins were found in the $S_1 \leftarrow S_0$ spectrum, corresponding to the phenol molecule acting as a proton donor or as an acceptor in the hydrogen bond [10]. Vibrational spectroscopies in the O–H stretching region also indicated that the dimer has one hydrogen bond [11,12]. The geometry of the dimer obtained by rotational coherence spectroscopy is not of a planar one as suggested previously [13], but is distorted due to an attractive interaction between the phenyl rings [14]. The phenol dimer was

also studied by MPI-photoelectron spectroscopy [15]. Two different IEs were reported: one for the donor and one for the acceptor. The most recent values obtained by zero-kinetic-energy (ZEKE) photoelectron spectroscopy are 63649 ± 4 and $\approx 64300 \text{ cm}^{-1}$ for the donor and the acceptor, respectively [16]. The ZEKE spectroscopy also suggested a significant strengthening of the hydrogen bond (shortening of the bond length) on ionization.

In this letter we report the electronic spectra of $(\text{C}_6\text{H}_5\text{OH})_2^+$. Compared with other aromatic dimer ions, features characteristic of $(\text{C}_6\text{H}_5\text{OH})_2^+$ are summarized as follows. Two components can be distinguished in $(\text{C}_6\text{H}_5\text{OH})_2^+$, although they are the same molecules. The positive charge may be localized on the donor part, since the IE of the donor is by 0.08 eV (650 cm^{-1}) lower than that of the acceptor. The O–H \cdots O hydrogen bond may prevent the two phenyl rings from taking a parallel configuration suitable for the resonance interaction.

2. Experimental

The experiment was carried out by using a cluster beam apparatus with a reflectron-type time-of-flight (TOF) mass spectrometer [17]. Neutral clusters were formed by expanding a mixture of sample and argon gas through a pulsed valve. After passing through a skimmer and a collimator, the cluster beam entered the acceleration region of the mass spectrometer. A pulsed ionization laser ($\lambda_i = 210 \text{ nm}$) intersected the cluster beam, where the parent ions were produced by 2-photon ionization of the neutral clusters. While traveling in the acceleration region, the prepared ions were excited by a pulsed dissociation laser ($\lambda_d = 340\text{--}1400 \text{ nm}$). The 2-photon ionization at 210 nm leads to large excess energy, producing hot cluster ions. However, such hot ions lose large parts of the internal energies instantaneously by evaporating neutral molecules in the focus of the ionization laser. The dimer ions probed by the dissociation laser came from larger clusters through evaporative cooling processes; the temperature of the ions was not so high as anticipated from the excess energy. After secondary acceleration, both the remaining parent ions and the photofragment ions were introduced into an ion-drift chamber of the mass spectrometer. The ions were then reflected by a two-stage ion reflector and detected by dual microchannel plates.

We used two methods to obtain the electronic spectra of $(\text{C}_6\text{H}_5\text{OH})_2^+$. One method was

based on the detection of the fragment ion. In this case, the carrier gas was passed over phenol placed in the head of the heated nozzle (≈ 80 °C). The dissociation laser was introduced at 3–4 mm downstream from the ionization laser; the length was sufficient to selectively excite the dimer ion. Only $C_6H_5OH^+$ was found as the fragment ion from $(C_6H_5OH)_2^+$. Therefore the photodissociation spectrum was obtained from the yield of $C_6H_5OH^+$ as a function of wavelength. The other method was the measurement of photodepletion efficiency of $(C_6H_5OH)_2^+$ relative to that of $(C_6H_6)_2^+$. The pre-expansion mixture was prepared by bubbling the carrier gas through the solution of phenol in benzene. Figure 1 displays the dimer ion region of TOF mass spectra of cluster ions produced from a mixture of phenol and benzene. The spectrum obtained without λ_d is shown in Fig. 1a. Three peaks are assigned to benzene dimer (B_2^+), benzene–phenol hetero-dimer (BP^+) and phenol dimer (P_2^+) ions. In order to excite all three ions simultaneously, the dissociation laser was introduced at only 0.5 mm downstream from the ionization laser. The spectrum obtained with λ_d (423 nm) is shown in Fig. 1b. Approximately 40 % of the $(C_6H_6)_2^+$ ion signals disappeared by the introduction of λ_d . Similar depletion is also seen for $(C_6H_6 \cdots C_6H_5OH)^+$ and $(C_6H_5OH)_2^+$, indicating that the dissociation cross sections of these ions are also appreciable at $\lambda_d = 423$ nm. From the measurement we can estimate the cross sections of $(C_6H_5OH)_2^+$ relative to $(C_6H_6)_2^+$. Since we have already known the cross section of $(C_6H_6)_2^+$ as a function of wavelength [3,4], we can obtain the spectral feature of the photodepletion efficiency of $(C_6H_5OH)_2^+$.

3. Results and discussion

3.1. Photofragment yield spectrum of $(C_6H_5OH)_2^+$

Figure 2 exhibits the electronic spectrum of $(C_6H_5OH)_2^+$ (open circles) in the region of 338–434 nm. The photodissociation cross sections at a series of wavelengths were obtained from the intensities of $C_6H_5OH^+$ normalized according to the dissociation laser power. The measurement performed with a given laser dye was scaled to the others based on the cross sections determined in overlapping regions of the dye gain curves. The error bars indicate one standard deviation of statistical uncertainties determined from repeated dye laser scans. The

spectrum of $(\text{C}_6\text{H}_5\text{OH})_2^+$ shows a broad band with small humps at ≈ 380 and ≈ 394 nm.

Mikami and co-workers studied hydrogen-bonded complex ions of phenol with several other molecules [18–21]. They recorded electronic spectra of these ions in the 350–460 nm region. For $(\text{C}_6\text{H}_5\text{OH}\cdots\text{NH}_3)^+$ and $[\text{C}_6\text{H}_5\text{OH}\cdots\text{N}(\text{CH}_3)_3]^+$, the spectra showed well-resolved vibronic structures characteristic of the phenoxy radical, $\text{C}_6\text{H}_5\text{O}$. The result suggests that the complex ions consist of $\text{C}_6\text{H}_5\text{O}$ with H^+NH_3 or $\text{H}^+\text{N}(\text{CH}_3)_3$ and that the $\text{C}_6\text{H}_5\text{O}$ unit acts as a chromophore for the electronic transition. On the other hand, the spectrum of $(\text{C}_6\text{H}_5\text{OH}\cdots\text{Ar})^+$ exhibited a structureless band at around 385 nm. The band was unambiguously attributed to the $\text{C} \leftarrow \text{X}$ transition of the phenol ion, $\text{C}_6\text{H}_5\text{OH}^+$, because the proton transfer to argon atom was not expected. The spectra of $(\text{C}_6\text{H}_5\text{OH}\cdots\text{H}_2\text{O})^+$ and $(\text{C}_6\text{H}_5\text{OH}\cdots p\text{-dioxane})^+$ showed broad bands similar to that of $(\text{C}_6\text{H}_5\text{OH}\cdots\text{Ar})^+$. The result implies that these complex ions consist of $\text{C}_6\text{H}_5\text{OH}^+$ with H_2O or p -dioxane and that the broad bands are due to the $\text{C} \leftarrow \text{X}$ transition of the $\text{C}_6\text{H}_5\text{OH}^+$ chromophore.

The spectrum of $(\text{C}_6\text{H}_5\text{OH})_2^+$ shown in Fig. 2 is essentially the same with those of the hydrogen-bonded complex ions with the $\text{C}_6\text{H}_5\text{OH}^+$ chromophore. The similarity indicates that the band arises from the $\text{C} \leftarrow \text{X}$ transition of the $\text{C}_6\text{H}_5\text{OH}^+$ chromophore in $(\text{C}_6\text{H}_5\text{OH})_2^+$. The equilibrium structure of $(\text{C}_6\text{H}_5\text{OH})_2^+$ is composed of a phenol ion and a neutral phenol; the charge is localized on the proton-donating phenol as indicated in the inset of Fig. 2. However, positions of the small humps on the spectrum of $(\text{C}_6\text{H}_5\text{OH})_2^+$ (394 and 380 nm) almost coincide with those of the 0–0 band (395 nm) and the most intense vibronic band (380 nm) of $(\text{C}_6\text{H}_5\text{OH}\cdots\text{NH}_3)^+$ [19]. The $(\text{C}_6\text{H}_5\text{OH})_2^+$ ions prepared by our method may contain a small amount of structural isomers having the $\text{C}_6\text{H}_5\text{O}$ chromophore.

3.2. Photodepletion spectrum of $(\text{C}_6\text{H}_5\text{OH})_2^+$

The main subject of the present work is to characterize the interaction between the two phenyl rings in $(\text{C}_6\text{H}_5\text{OH})_2^+$. The electronic spectrum in near-infrared wavelength region is helpful to understand the nature of the interaction. The spectra of homo-dimer ions of benzene [3,4], toluene [5] and p -difluorobenzene [22] show intense CR bands in this region. For each homo-dimer ion, the CR transition energy was found to be just twice of the binding energy,

suggesting that the dominant contribution to the binding energy is from the resonance interaction [4]. If the resonance interaction between the two phenyl rings is also dominant in $(\text{C}_6\text{H}_5\text{OH})_2^+$, then we can expect a CR band of this ion with appreciable intensity.

Figure 3 displays the overall spectrum of $(\text{C}_6\text{H}_5\text{OH})_2^+$. The open circles in the regions of 338–434 and 530–670 nm were obtained from the yield of the fragment ion; the results in the former region were discussed in the previous section. The closed circles in the 440–1400 nm region were obtained from the depletion efficiency of $(\text{C}_6\text{H}_5\text{OH})_2^+$. The spectrum of $(\text{C}_6\text{H}_6)_2^+$ is also shown by the dotted curve for reference. The ordinate stands for the cross section relative to the maximum of $(\text{C}_6\text{H}_6)_2^+$ at 920 nm. At the wavelengths where the cross section of $(\text{C}_6\text{H}_6)_2^+$ is fairly large, we should reduce the power of the dissociation laser in order to avoid saturation; the experimental uncertainties are large in the 800–1100 nm region. No intense band is observed on the spectrum of $(\text{C}_6\text{H}_5\text{OH})_2^+$ except for the $\text{C} \leftarrow \text{X}$ transition at around 390 nm. Although weak features are seen in the regions of 500–650 and 750–1100 nm, the cross sections are at most 4 % of the maximum cross section of $(\text{C}_6\text{H}_6)_2^+$.

Since the IE of the donor ring is by 0.08 eV lower than that of the acceptor ring [16], the positive charge may be localized on the donor ring in $(\text{C}_6\text{H}_5\text{OH})_2^+$. The charge localization is unfavorable for the resonance interaction between the two rings and consequently reduces the intensity of the CR band. However, we have found that the resonance-type interaction is also important in the $(\text{C}_6\text{H}_6 \cdots \text{C}_6\text{H}_5\text{CH}_3)^+$ hetero-dimer ion [8], despite the large difference in the IEs (0.415 eV) between benzene and toluene. For $(\text{C}_6\text{H}_5\text{OH})_2^+$, the difference in IEs is not large enough to account for the lack of the CR band.

In order to explain the strong CR interaction observed in $(\text{C}_6\text{H}_6)_2^+$ and probably in $(\text{C}_6\text{H}_6 \cdots \text{C}_6\text{H}_5\text{CH}_3)^+$, we favor parallel or approximately parallel configurations of the two aromatic rings for these ions which allow π overlap between the two rings. The geometry of $(\text{C}_6\text{H}_5\text{OH})_2$ has not been determined conclusively yet, let alone $(\text{C}_6\text{H}_5\text{OH})_2^+$. Felker and co-workers proposed a nonplanar geometry for $(\text{C}_6\text{H}_5\text{OH})_2$ with the two aromatic rings interacting in a way that maximizes the atom–atom contact between them subject to the geometrical constraint of the hydrogen bond [14]. The ZEKE photoelectron spectroscopy suggested a significant strengthening of the hydrogen bond on ionization [16]. The strong hydrogen bond

in $(\text{C}_6\text{H}_5\text{OH})_2^+$ probably prevents the two rings from taking a parallel configuration. Therefore we expect that the resonance interaction is less significant in $(\text{C}_6\text{H}_5\text{OH})_2^+$ and that the CR band (if any) is much weaker than that of $(\text{C}_6\text{H}_6)_2^+$.

The lack of the CR band indicates that the charge in $(\text{C}_6\text{H}_5\text{OH})_2^+$ is not shared with the two component molecules. If the positive charge stays always on the donor ring, the dominant contribution to the binding energy of $(\text{C}_6\text{H}_5\text{OH})_2^+$ is from the charge–dipole interactions between the two phenyl rings and through the hydrogen bond [16].

3.3. Size dependence of photodissociation cross sections

The photodissociation cross sections of $(\text{C}_6\text{H}_5\text{OH})_n^+$ were measured as functions of cluster sizes at several wavelengths. Figure 4 shows the results at 380 and 818 nm. The ordinate stands for the cross sections relative to that of $(\text{C}_6\text{H}_5\text{OH})_2^+$ at each wavelength. At 380 nm, which corresponds to the $\text{C} \leftarrow \text{X}$ band of $(\text{C}_6\text{H}_5\text{OH})_2^+$, the magnitude of the cross section was found to be almost independent of cluster size. At 818 nm, however, the cross section increases linearly from $n = 2$ to 5 and then remains almost constant from $n = 5$ to 7. The cross section of $(\text{C}_6\text{H}_5\text{OH})_5^+$ is approximately three times as large as that of $(\text{C}_6\text{H}_5\text{OH})_2^+$.

Recently, Fujii et al. measured infrared spectra of $(\text{C}_6\text{H}_5\text{OH})_n^+$ with $n = 2\text{--}4$ and found intense bands at the frequencies characteristic of the O–H group free from the hydrogen bond [23]. The result rules out a cyclic (ring) structure for $(\text{C}_6\text{H}_5\text{OH})_n^+$, where all the O–H groups are involved in the hydrogen bonds, and supports an open chain structure. Let us assume that the charge stays on the phenol molecule at the end of a flexible chain. If the chain becomes long, the charged molecule has much chance to be in a parallel configuration with the molecule at the other end of the chain. This explanation is consistent with the observed increase in the cross section with cluster size. The degree of parallel overlap of the two molecules may be maximized at cluster size of $n = 5$. However, the cross section of $(\text{C}_6\text{H}_5\text{OH})_5^+$ is smaller than that of $(\text{C}_6\text{H}_6)_2^+$ by a factor of about 10. The distance must be too long for the two molecules at both ends of the $(\text{C}_6\text{H}_5\text{OH})_5^+$ chain to effectively interact with each other.

In conclusion we have shown that the charge resonance interaction between two aromatic rings seems to be insignificant when they cannot be in a parallel configuration. As a

result, the positive charge in $(\text{C}_6\text{H}_5\text{OH})_2^+$ is not shared with the two component molecules, in contrast to $(\text{C}_6\text{H}_6)_2^+$ and other homo-dimer ions. For larger $(\text{C}_6\text{H}_5\text{OH})_n^+$ ions, location of the charged phenol molecule(s) in the clusters is still in question. Further spectroscopic studies are necessary to make this point clear.

References

- [1] E. J. Bieske and J. P. Maier, *Chem. Rev.* 93 (1993) 2603.
- [2] J. M. Farrar, in: *Cluster Ions*, eds. C. Y. Ng, T. Baer and I. Powis (John Wiley & Sons, Chichester, 1993), p. 243.
- [3] K. Ohashi and N. Nishi, *J. Phys. Chem.* 96 (1992) 2931.
- [4] K. Ohashi, Y. Nakai, T. Shibata and N. Nishi, *Laser Chem.* 14 (1994) 3.
- [5] Y. Inokuchi, K. Ohashi, T. Shibata and N. Nishi, in preparation.
- [6] Y. Inokuchi, K. Ohashi, M. Matsumoto and N. Nishi, *J. Phys. Chem.* 99 (1995) 3416.
- [7] M. S. El-Shall and M. Meot-Ner (Mautner), *J. Phys. Chem.* 91 (1987) 1088.
- [8] K. Ohashi, Y. Nakai, T. Shibata, Y. Inokuchi and N. Nishi, *Proc. of Yamada Conf. XLIII* (1995) in press.
- [9] K. Fuke and K. Kaya, *Chem. Phys. Letters* 91 (1982) 311.
- [10] K. Fuke and K. Kaya, *Chem. Phys. Letters* 94 (1983) 97.
- [11] G. V. Hartland, B. F. Henson, V. A. Venturo and P. M. Felker, *J. Phys. Chem.* 96 (1992) 1164.
- [12] T. Ebata, T. Watanabe and N. Mikami, *J. Phys. Chem.* 99 (1995) 5761.
- [13] M. Ito, *J. Mol. Spectrosc.* 4 (1960) 125.
- [14] L. L. Connell, S. M. Ohline, P. W. Joireman, T. C. Corcoran and P. M. Felker, *J. Chem. Phys.* 96 (1992) 2585.
- [15] K. Fuke, H. Yoshiuchi, K. Kaya, Y. Achiba, K. Sato and K. Kimura, *Chem. Phys. Letters* 108 (1984) 179.
- [16] O. Dopfer, G. Lembach, T. G. Wright and K. Müller-Dethlefs, *J. Chem. Phys.* 98 (1993) 1933.
- [17] K. Ohashi and N. Nishi, *J. Chem. Phys.* 95 (1991) 4002.
- [18] N. Mikami, T. Sasaki and S. Sato, *Chem. Phys. Letters* 180 (1991) 431.
- [19] N. Mikami, S. Sato and M. Ishigaki, *Chem. Phys. Letters* 202 (1993) 431.
- [20] S. Sato, T. Ebata and N. Mikami, *Spectrochim. Acta* 50A (1994) 1413.
- [21] N. Mikami, *Bull. Chem. Soc. Jpn.* 68 (1995) 683.

- [22] M. Fujii, K. Ohtsuka and M. Ito, unpublished results.
- [23] A. Fujii, T. Sawamura, K. Yoshida, A. Iwasaki, S. Sato, T. Ebata and N. Mikami,
Abstract of NAIR Workshop on Cluster Science, Tsukuba (1996) p. 6.

Figure Captions

Fig. 1. TOF mass spectra showing photodepletion behavior of $(\text{C}_6\text{H}_6)_2^+$ (labeled B_2^+), $(\text{C}_6\text{H}_6 \cdots \text{C}_6\text{H}_5\text{OH})^+$ (BP^+) and $(\text{C}_6\text{H}_5\text{OH})_2^+$ (P_2^+) with the photodissociation laser off (a) and with the laser on at $\lambda_d = 423$ nm (b).

Fig. 2. Photofragment yield spectra of $(\text{C}_6\text{H}_5\text{OH})_2^+$ (open circles) and $(\text{C}_6\text{H}_6)_2^+$ (dotted curve). The inset shows an estimated structure of $(\text{C}_6\text{H}_5\text{OH})_2^+$ composed of a phenol ion and a neutral phenol.

Fig. 3. Overall photodissociation spectrum of $(\text{C}_6\text{H}_5\text{OH})_2^+$. The open circles are the data obtained from the yield of $\text{C}_6\text{H}_5\text{OH}^+$; the closed circles are from the photodepletion efficiency of $(\text{C}_6\text{H}_5\text{OH})_2^+$. The ordinate stands for the cross section relative to the maximum of $(\text{C}_6\text{H}_6)_2^+$ at 920 nm. The dotted curve is the spectrum of $(\text{C}_6\text{H}_6)_2^+$ for reference.

Fig. 4. Photodissociation cross sections of $(\text{C}_6\text{H}_5\text{OH})_n^+$ as a functions of cluster size (n) at $\lambda_d = 380$ (circles) and 818 nm (squares). The ordinate stands for the cross section ($\sigma(n)$) relative to that of $(\text{C}_6\text{H}_5\text{OH})_2^+$ ($\sigma(2)$) at each wavelength.

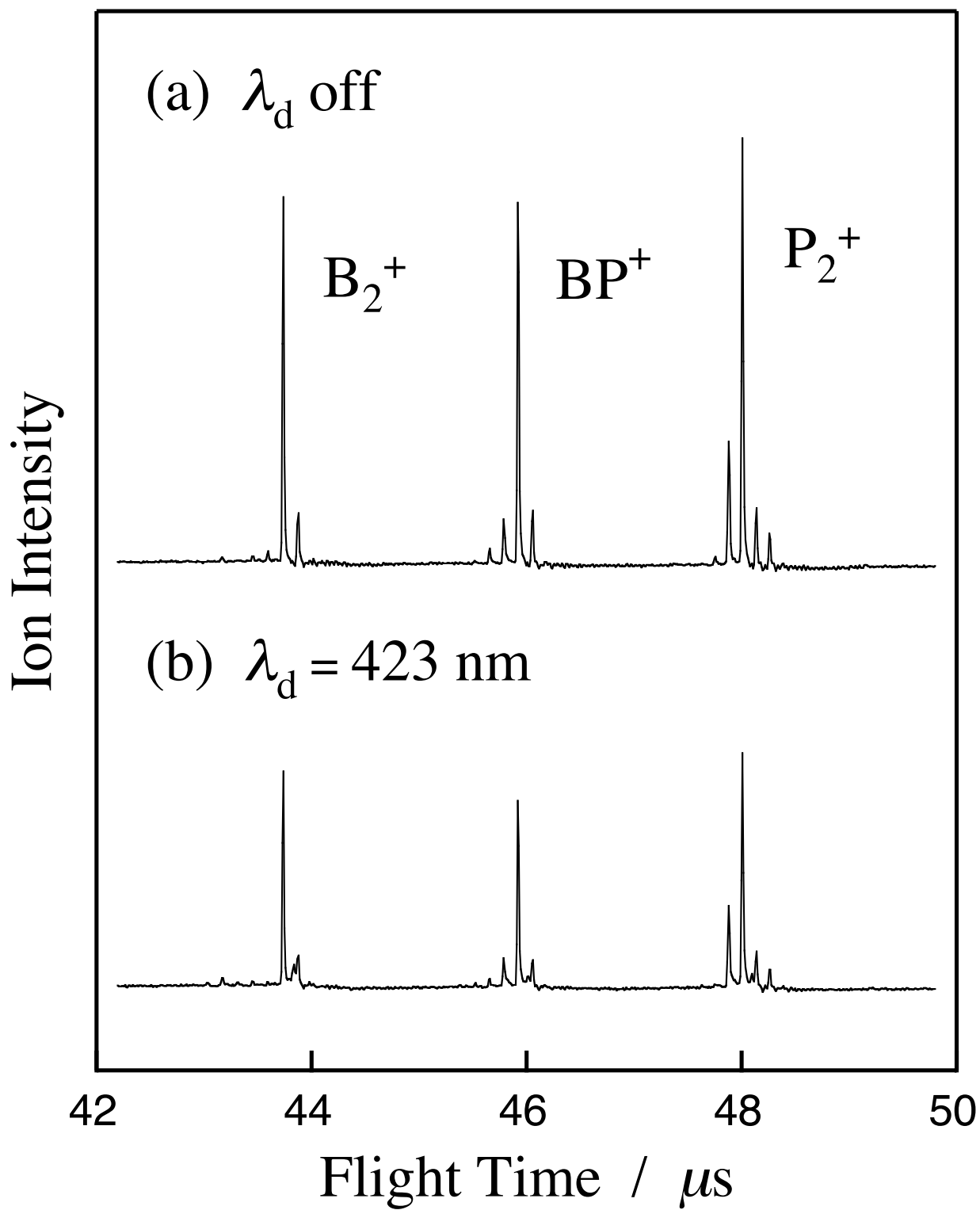


Fig. 1. Ohashi *et al.*

Cross Section

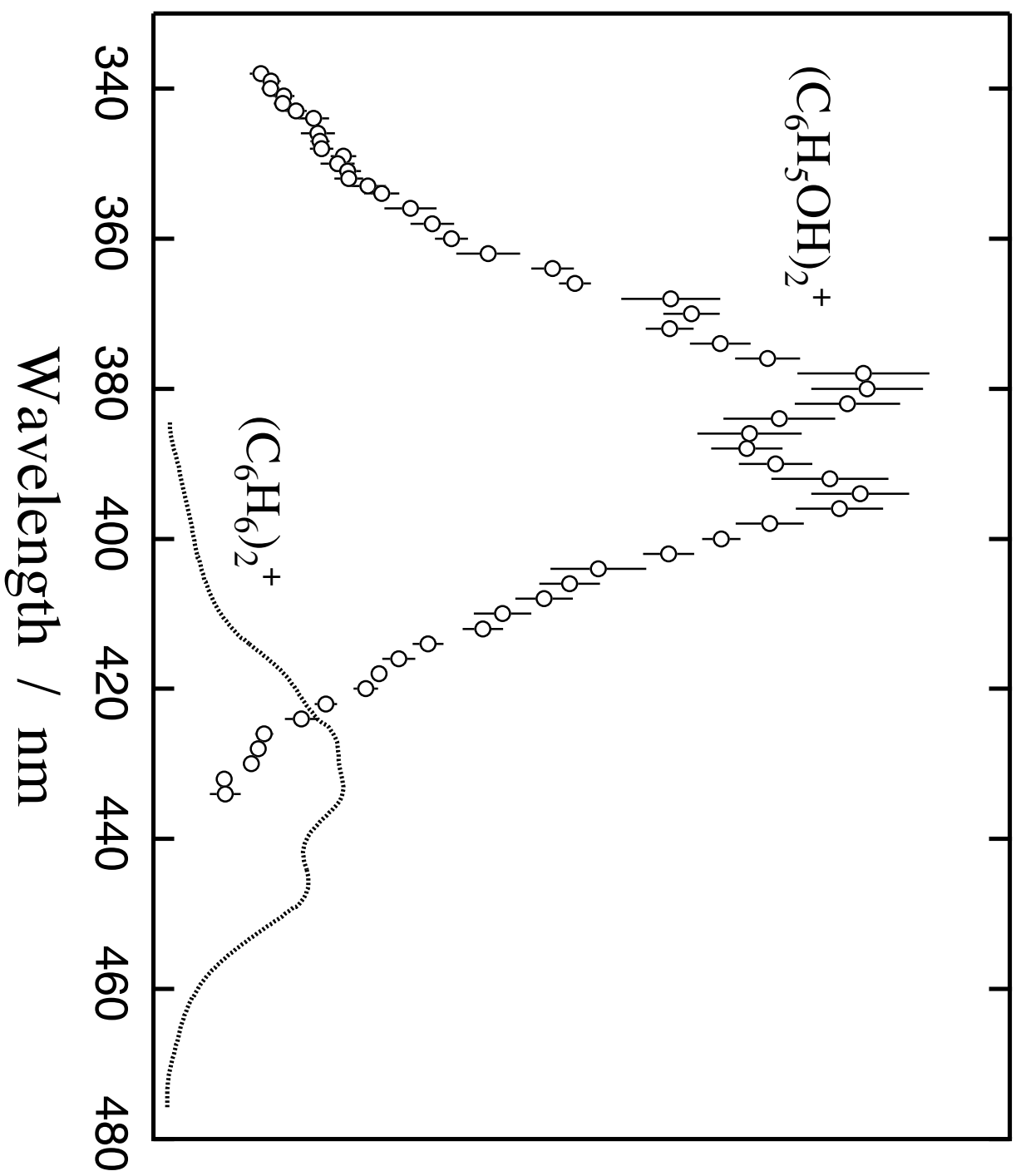


Fig. 2. Ohashi *et al.*

Relative Cross Section

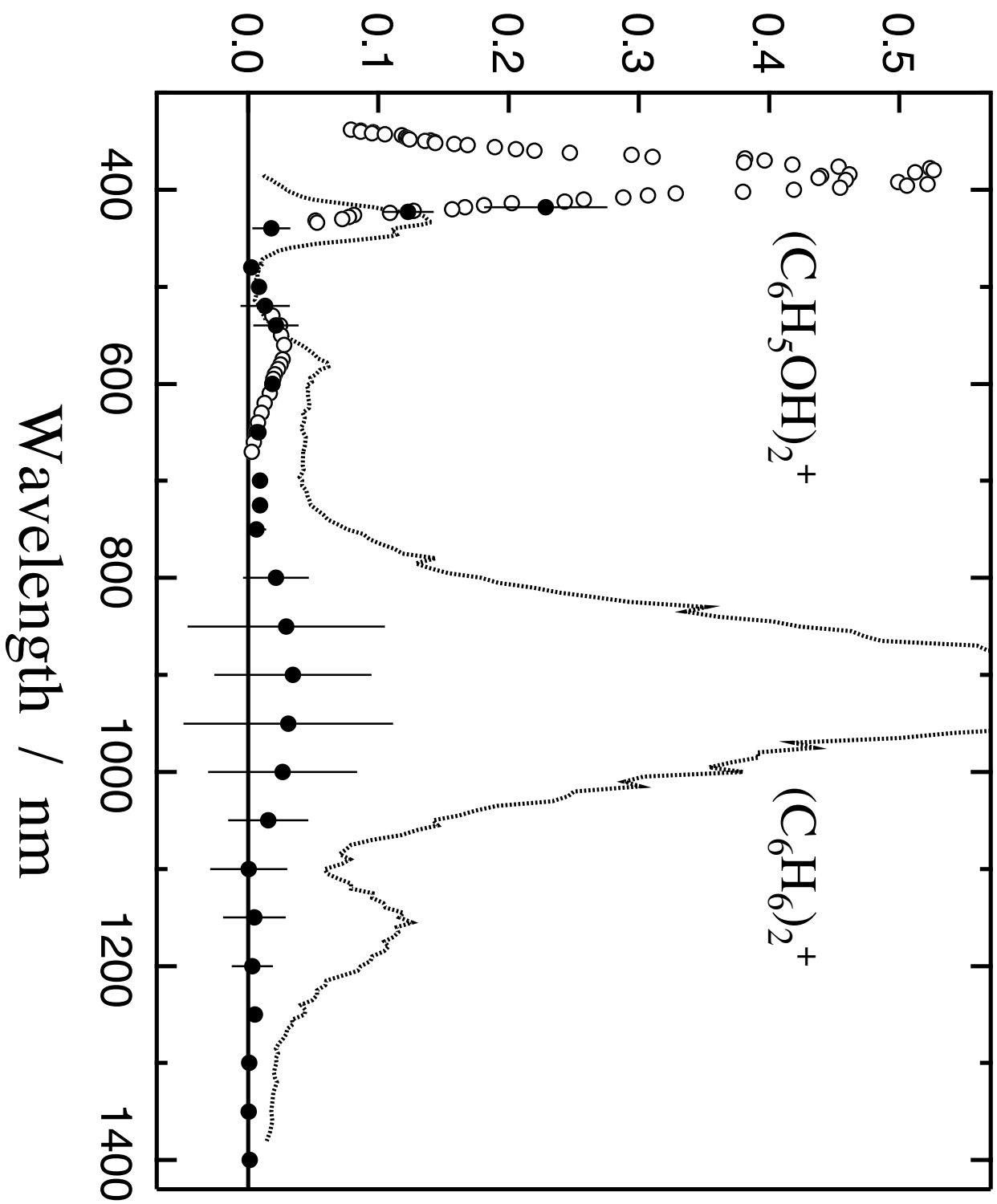


Fig. 3. Ohashi *et al.*

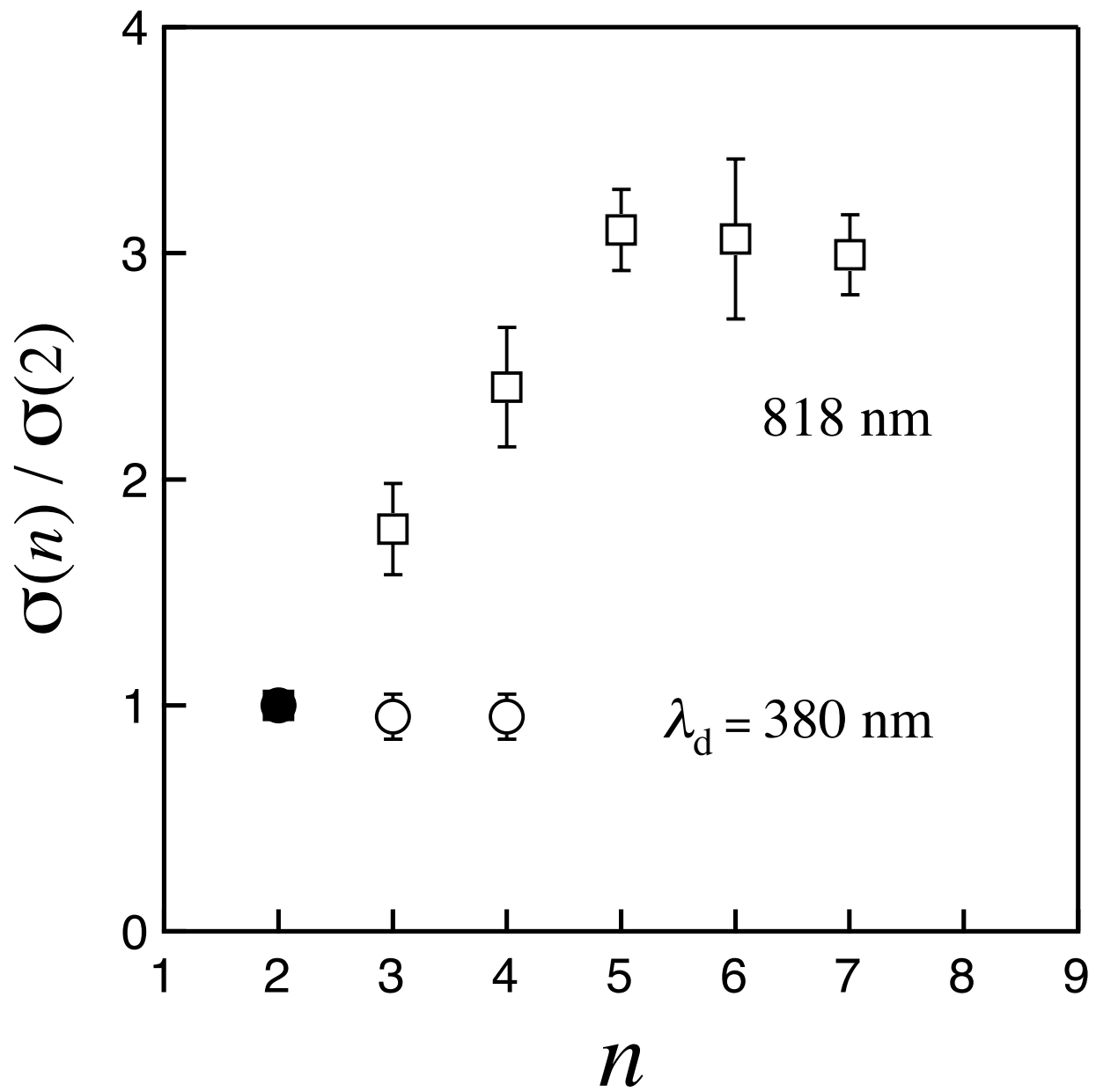


Fig. 4. Ohashi *et al.*